International Journal of Mechanical, Industrial and Aerospace Sciences
ISSN: 2517-9950
Vol:8, No:5, 2014

Design and Analysis of Flexible Slider Crank Mechanism

Thanh-Phong Dao, Shyh-Chour Huang

***Abstract*—**This study presents the optimal design and formulation of a kinematic model of a flexible slider crank mechanism. The objective of the proposed innovative design is to take extra advantage of the compliant mechanism and maximize the fatigue life by applying the Taguchi method. A formulated kinematic model is developed using a pseudo-rigid-body model (PRBM). By means of mathematic models, the kinematic behaviors of the flexible slider crank mechanism are captured using MATLAB software. Finite element analysis (FEA) is used to show the stress distribution. The results show that the optimal shape of the flexible hinge includes a force of 8.5*N*, a width of 9*mm* and a thickness of 1.1*mm*. Analysis of variance shows that the thickness of the proposed hinge is the most significant parameter, with an F test of 15.5. Finally, a prototype is manufactured to prepare for testing the kinematic and dynamic behaviors.

***Keywords*—**Kinematic behavior, fatigue life, pseudo-rigid-body model, flexible slider crank mechanism.

I. Introduction

COMPLIANT mechanisms or flexible mechanisms are cataloged as those mechanisms which gain mobility from their links and flexible hinges, rather than the use of traditional kinematic pairs. The design of compliant mechanisms, as compared to conventional mechanisms, requires only a small scale of translation or angular rotation to achieve particular advantages, such as non-friction, no need for lubrication, ease of fabrication and no need for maintenance. With this in mind, a flexible slider crank mechanism was developed in this study as a replacement for a traditional slider crank mechanism. Tanık [1] investigated the transmission angle of a compliant slider crank mechanism via two theorems. However, while the flexure hinge has many advantages, during the performance process the displacement/deflection is always subject to stress at the pivot joint. As a result, the desired structure will have a failure, called fatigue failure. Fatigue failure plays a most significant role in machine design; therefore, it should be given serious consideration. Dirksen et al. [2] presented the fatigue life of a variety of flexible hinges with rectangular, circular and parabolic profile geometries. Their results showed that circular hinges provided a safer design than other hinges.

For these reasons, the logical question is how circular flexural hinges can be designed to prevent fatigue failure. Thus, this aim of this research was to develop an innovative design which would maximize the fatigue life of the flexible slider crank mechanism. In the past handling of such problems, there has been increasing interest in such optimal procedures as the Taguchi method, genetic algorithms and fuzzy logic controllers, which are used in almost all industrial fields. The Taguchi method is the most useful as it is capable of optimizing individual objectives separately because of the reduced number of experiments. Javadi et al. [3] optimized residual stresses produced by friction stir welding using the Taguchi method.

In addition, flexible hinges and links always undergo a large deflection during their motion; therefore, there is a need to model the kinematics that capture and predict more accurately their deflected shape. In past decades, several approaches have been developed to analyze the kinematic and dynamic behaviors of compliant links. Tari and Su [4] made an effort to formulate kinematic equations of a compliant four-bar mechanism based on function, motion and path generations. More recently, in 2013, a kinematic model was established by Bauchau and Han [5] using finite deformation measures. While these approaches were helpful, they were not easy to carry out. The concept of the pseudo-rigid-body model has since been developed by Howell [6] for analyzing the kinematic behavior of flexible mechanisms. This method assumes that flexible hinges behave as revolute joints with torsional springs attached, while the thicker sections of the mechanism behave as rigid links. Using this approach, compliant mechanisms can be analyzed and designed using well-established traditional rigid-body mechanism theory.

This paper presents an optimal design and describes the kinematic behavior of a flexible slider crank mechanism. First, an innovative design was developed using the concept of the compliant mechanism. Next, the Taguchi method was applied to maximize fatigue life by finding the optimal parameters. Mathematic models were then formulated to capture the kinematic behavior, and finite element analysis (FEA) was used to estimate the stress distribution. Finally, a real model was manufactured to test the kinematic and dynamic behaviors.

II. Modeling of Flexible Slider Crank Mechanism

Fig. 1 illustrates a traditional slider crank mechanism. The relative rotation takes place between the links by means of conventional kinematic joints. The innovative-design modeling of this mechanism, called a flexible slider crank mechanism, is given in Fig. 2, including three flexure hinges with small dimensions for both thickness and width. These hinges produce a rotational motion output similar to that of traditional joints, or the same function; the only difference is that a rotational center is no longer collocated. As noted in a previous study by Dirksen and Lammering [7], rectangular cross-section flexible hinges have low bending stiffness with very high rotational deflection, circular cross-section flexible hinges display medium bending stiffness with high rotational deflection and parabolic cross-section flexible hinges achieve high bending stiffness with low rotational deflection. In this study, a circular flexure

Shyh-Chour Huang and Thanh-Phong Dao are with the Department of Mechanical Engineering, National Kaohsiung University of Applied Sciences, Taiwan, ROC. (Corresponding author Tel.: (07)-3814526 ext 5313; fax: (07)-3831373. e-mail address: shuang@cc.kuas.edu.tw).

hinge was selected in order to take advantage of its being a single-axis flexure hinge with a large deflection and low bending stiffness. The sectional dimensions of the proposed circular flexible hinge were the width (w) and the thickness (t), as shown in Fig. 3. There was one degree of freedom for the rotational motion about the z-axis. The flexible slider crank mechanism was made of an aluminum wrought alloy, because of its high fatigue strength and elastic properties.

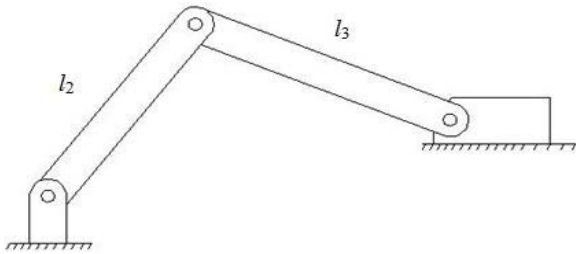

Fig. 1 Traditional slider crank mechanism

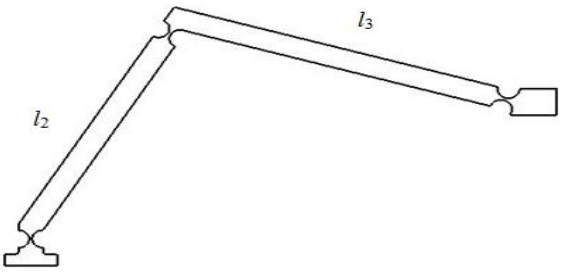

Fig. 2 Innovative-design modeling of slider crank flexible mechanism

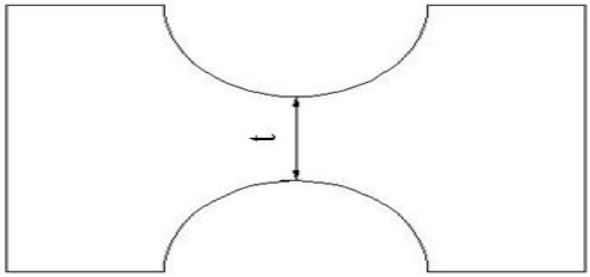

Fig. 3 Cross section of circular flexural hinge

III. Fatigue Strength of Circular Flexural Hinges

Flexible members are required for multiple motions, up to many millions of cycles or even infinite life. Such repeated loading causes fluctuating stresses in members, which can result in fatigue failure at stresses that are less than those which cause static failure. Fatigue is the most common failure of a component as a result of being subjected to repeated or cyclic/fluctuating stress, called dynamic loading. For these and other reasons, in order to achieve the optimal geometry of circular flexural hinges for the safety factor, the fatigue strength should be analyzed and determined in the design process. Along with the emergence of fatigue theories, several models are now available for fatigue failure prediction. The stress-life model is appropriate for components that undergo fluctuating stresses. Another model is the fracture-mechanics approach, which can be used for other components, such as airplane wings, that are subject to randomly varying stresses.

The fatigue life mainly depends on two stresses: mean stress and alternative stress. It also depends on the stress concentration factor, the surface effect (scratches, sharp transitions and edges), notch effect, etc. Here it has been assumed that all loads are time-harmonic with a constant amplitude, in consideration of the limitations of this study regarding the effect of mean stress and alternative stress on fatigue strength.

A. Zero Mean Stress ($\delta_m = 0$)

Various methods have been used to estimate the fatigue strength in the absence of mean stress ($\delta_m = 0$). A traditional method is briefly described in the following linear equation:

$$S_f = \beta S_{ut} \tag{1}$$

where S_f is the fatigue strength and S_{ut} is the ultimate strength of a material. The factors $\beta = 0.5$ for steel and titanium alloys and $\beta = 0.35$ for aluminum alloys are typically used.

B. Nonzero Mean Stress ($\delta_m \neq 0$)

In this case, there have been different criteria used in fatigue design as follows:

Soderberg [8]:

$$\frac{\delta_a}{S_f} + \frac{\delta_m}{S_y} = 1 \tag{2}$$

Modified Goodman [9]:

$$\frac{\delta_a}{S_f} + \frac{\delta_m}{S_{ut}} = 1 \tag{3}$$

Gerber [10]:

$$\frac{\delta_a}{S_f} + \left(\frac{\delta_m}{S_{ut}}\right)^2 = 1 \tag{4}$$

ASME-Elliptic:

$$\left(\frac{\delta_a}{S_f}\right)^2 + \left(\frac{\delta_m}{S_{ut}}\right)^2 = 1 \tag{5}$$

Langer first-cycle yielding:

$$\frac{\delta_a}{S_y} + \frac{\delta_m}{S_y} = 1 \tag{6}$$

Fig. 4 shows a fatigue diagram illustrating various criteria of failure. Of these criteria, Soderberg's is the most conservative due to the use of the yield strength of a material S_y, whereas Goodman and Gerber connect experimental data quite well, while ASME-Elliptic is less conservative. Recently, Dao and Huang [11] applied the modified Goodman criterion to predict the fatigue strength of the rectangular flexure hinge.

In the present work, the modified Goodman criterion was selected to analyze the fatigue life of the flexible slider crank mechanism, since the mechanism undergoes fluctuating stresses. By applying ANSYS commercial software, a nonlinear finite element analysis was carried out to find the results of the fatigue life cycles of the system.

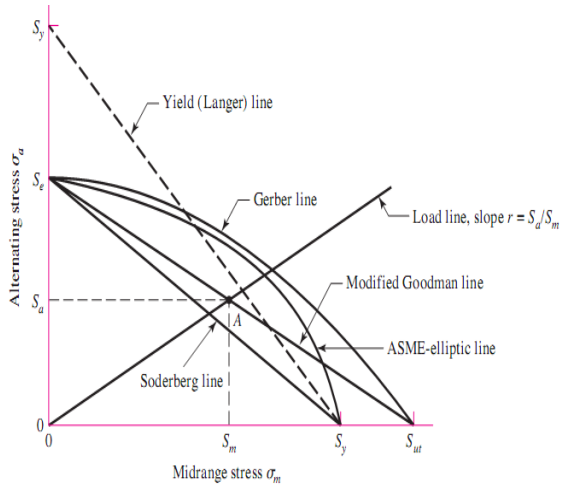

Fig. 4 Schematic diagram of various criteria of fatigue [12]

IV. Optimal Design of Circular Flexural Hinges

To ensure the safety and reliability of compliant mechanisms, fatigue failure is always the most important issue to be considered in machine design. In this study, the stress was a fluctuating stress with nonzero mean stress. Thus, the flexible slider crank mechanism would be at risk for fatigue failure during cycle-repeated motion. To obtain the desired relative rotation of the proposed flexure hinges, the optimal design required that their optimal sizes be determined. The objective function was the maximizing of the fatigue life of the flexible slider crank mechanism. To handle this problem, the Taguchi method was employed. In finding the optimal process parameter values based on a single quality characteristic, the Taguchi method is one of the most significant tools because it is an efficient experimental method which requires only a small number of experiments to measure the quality and analysis of the optimal process.

A. Taguchi Method

Taguchi method applications are concerned with the optimization of a single performance characteristic. The Taguchi method uses a special design of orthogonal arrays to study an entire parameter space with only a small number of experiments. The experimental results are then transformed into a signal-to-noise (S/N) ratio. The S/N ratio can be used to measure performance characteristics deviating from the desired values. Usually, there are three categories of performance characteristics in the analysis of the S/N ratio: the lower-the-better, the higher-the-better and the nominal-the-better. In this study, an L_9 orthogonal array experiment was used because there are three parameters and three levels. To obtain the optimal motion performance, the maximum fatigue life of a proposed mechanism is desired and, therefore, the higher-the-better fatigue should be selected. After determining the orthogonal array experiment and the number of parameter levels, the calculation for the S/N of the fatigue life can be made, as shown in the following equation.

The higher-the-better fatigue life is:

$$S/N_L = -10\log\left(\frac{1}{n}\sum_{i=1}^{n}\frac{1}{y_i^2}\right) \tag{7}$$

where y is the observed data.

B. Results and Discussion

The value of each of the process parameters was divided into three levels, as shown in Table I. Based on the Taguchi method, the L_9 orthogonal array with nine experiments and detailed values of each level is given in Table II. The results of fatigue life based on ANSYS software and their S/N ratio of the proposed mechanism are shown in Table III. The calculations of the mean of the S/N responses for fatigue life at each of the levels are shown in Table IV. As Fig. 5 illustrates, the optimal results were found in the 10th experiment, using a force of 8.5*N*, a width of 9*mm* and a thickness of 1.1*mm*; also, the optimized fatigue life was 1.8822e^6 cycles, in accordance with an S/N ratio of 125.49, as given in Table IV.

TABLE I
Parameters and Levels

Symbol	Parameters	Range	Unit	Level 1	Level 2	Level 3
A	Force	8.5-9.5	N	8.5	9	9.5
B	Width *w*	9-11	mm	9	10	11
C	Thickness *t*	0.9-1.1	mm	0.9	1	1.1

TABLE II
Experiment Layout Using an L_9 Orthogonal Array

Experiments	A	B	C
Number	Force (*N*)	Width *w* (*mm*)	Thickness *t* (*mm*)
1	1	1	1
2	1	2	2
3	1	3	3
4	2	1	2
5	2	2	3
6	2	3	1
7	3	1	3
8	3	2	1
9	3	3	2

TABLE III
NINE EXPERIMENTS WITH DETAILED VALUES AND RESULTS

No. Experiments	A Force (*N*)	B Width *w* (*mm*)	C Thickness *t* (*mm*)	Fatigue life (cycles)	S/N Ratio (*dB*)
1	8.5	9	0.9	10206	80.177
2	8.5	10	1	1.7926e^5	105.069
3	8.5	11	1.1	92203	99.294
4	9	9	1	85332	98.622
5	9	10	1.1	7.9777e^5	118.037
6	9	11	0.9	2095.9	66.427
7	9.5	9	1.1	6.277e^5	115.955
8	9.5	10	0.9	1793.7	65.076
9	9.5	11	1	53217	94.521
		Optimal results			
10	8.5	9	1.1	1.8822e^6	125.49

TABLE IV
MEAN OF S/N RESPONSES FOR FATIGUE LIFE

Symbol	Parameter	Mean of S/N Ratio (*dB*)			Max-Min
		Level 1	Level 2	Level 3	
A	Force	94.84	94.36	91.85	2.99
B	Width *w*	98.25	96.06	86.74	11.51
C	Thickness *t*	70.56	99.404	111.09	40.53
		Total mean = 93.68			

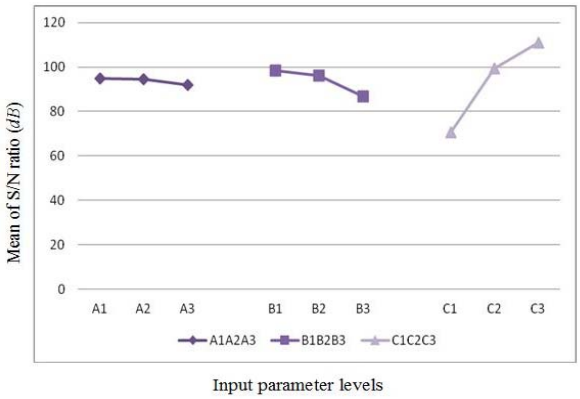

Fig. 5 Mean of S/N ratio for fatigue life

C. Analysis of Variance (ANOVA)

An analysis of variance (ANOVA) was performed to identify the process parameter that was most statistically significant in affecting the performance characteristics. Table V indicates that the thickness of the proposed hinge was the most significant parameter affecting the structure of the circular flexural hinge, with an F test of 15.5.

TABLE V
RESULTS OF ANOVA

Symbol	Parameters	DOF	SS	V	F
A	Force	2	15.5	7.75	1.33
B	Width *w*	2	223.8	111.9	1.33
C	Thickness *t*	2	2611.8	1305.9	15.5
Error		2	167.9	83.9	
Total		8	3019	1509.45	

V. KINEMATIC MODEL DEVELOPMENT

It is difficult to analyze nonlinear-large deflection using the Bernoulli-Euler theory. However, the recently developed pseudo-rigid-body model theory is an effective alternative for designing and analyzing nonlinear-large deflection by modeling a flexure hinge into two rigid links joined at a pin joint, with a torsional spring (including spring constants: k_1, k_2, k_3) located at the rotating center, as shown in Fig. 6. This section shows the formulation of the kinematic equations, through the application of the pseudo-rigid-body model and the geometric relations between links, assuming that α_2 is the rotational input angle; the length of link 2, $l_2 = 100mm$; and the length of link 3, $l_3 = 127mm$.

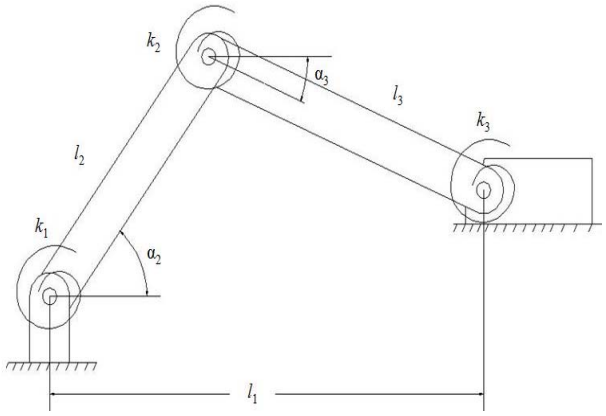

Fig. 6 Pseudo-rigid-body model of slider crank flexible mechanism

A. Position Analysis

Vector loop equation for flexible slider crank mechanism is:

$$l_1 = l_2 + l_3 \tag{8}$$

$$l_2 + l_3 - l_1 = 0 \tag{9}$$

$$l_2 e^{j\alpha_2} + l_3 e^{j\alpha_3} - l_1 e^{j\alpha_1} = 0 \tag{10}$$

Euler equation is described as:

$$e^{j\alpha_i} = \cos\alpha_i + j\sin\alpha_i \tag{11}$$

using Euler equivalents results in:

$$l_2(\cos\alpha_2 + j\sin\alpha_2) + l_3(\cos\alpha_3 + j\sin\alpha_3) - l_1(\cos\alpha_1 + j\sin\alpha_1) = 0 \tag{12}$$

Separating real and imaginary parts results in:

$$l_2\cos\alpha_2 + l_3\cos\alpha_3 - l_1\cos\alpha_1 = 0 \tag{13}$$

$$l_2 j\sin\alpha_2 + l_3 j\sin\alpha_3 - l_1 j\sin\alpha_1 = 0 \tag{14}$$

$$l_1 = l_2\cos\alpha_2 + l_3\cos\alpha_3 \tag{15}$$

$$\sin\alpha_3 = -\frac{l_2}{l_3}\sin\alpha_2 \tag{16}$$

$$\cos\alpha_3 = \frac{1}{l_3}\sqrt{l_3^2 - l_2^2\sin^2\alpha_2} \tag{17}$$

B. Velocity Analysis

Differentiating (10) with respect to time, where l_2, l_3 and α_1 are constants, the velocity of slider $\dot{l}_1$ varies with time:

$$jl_2e^{j\alpha_2}\dot{\alpha}_2 + jl_2e^{j\alpha 3}\dot{\alpha}_3 - \dot{l}_1 = 0 \tag{18}$$

The absolute velocity of link 2:

$$v_2 = jl_2e^{j\alpha_2}\dot{\alpha}_2 \tag{19}$$

The velocity difference of link 3 with respect to link 2:

$$v_{32} = jl_2e^{j\alpha_3}\dot{\alpha}_3 \tag{20}$$

Velocity of slider:

$$v_1 = \dot{l}_1 = v_2 + v_{32} \tag{21}$$

$$jl_2\dot{\alpha}_2\left(\cos\alpha_2 + j\sin\alpha_2\right) + jl_2\dot{\alpha}_3\left(\cos\alpha_3 + j\sin\alpha_3\right) - \dot{l}_1 = 0 \tag{22}$$

$$l_2\dot{\alpha}_2\left(j\cos\alpha_2 - \sin\alpha_2\right) + l_2\dot{\alpha}_3\left(j\cos\alpha_3 - \sin\alpha_3\right) - \dot{l}_1 = 0 \tag{23}$$

Separating real and imaginary parts results in:

$$\dot{\alpha}_3 = -\frac{l_2\dot{\alpha}_2\cos\alpha_2}{\sqrt{l_3^2 - l_2^2\sin^2\alpha_2}} \tag{24}$$

$$\dot{l}_1 = -l_2\dot{\alpha}_2\sin\alpha_2 - \frac{l_2^2\dot{\alpha}_2\sin\alpha_2\cos\alpha_2}{\sqrt{l_3^2 - l_2^2\sin^2\alpha_2}} \tag{25}$$

The absolute velocity of the centre of mass of link 2 results in:

$$v_{m2} = j\frac{l_2}{2}e^{j\alpha_2}\dot{\alpha}_2 \tag{26}$$

Substituting Euler equation and simplifying results in:

$$v_{m2} = \frac{1}{2}l_2\dot{\alpha}_2 \tag{27}$$

The absolute velocity of the centre of mass of link 3 results in:

$$v_{m3} = jl_2e^{j\alpha_2}\dot{\alpha}_2 + j\frac{l_3}{2}e^{j\alpha_3}\dot{\alpha}_3 \tag{28}$$

Substituting Euler equation and simplifying results in:

$$v_{m3} = \left[l_2^2\dot{\alpha}_2^2 + l_2l_3\cos\left(\alpha_2 - \alpha_3\right)\dot{\alpha}_2\dot{\alpha}_3 + \frac{1}{4}l_3^2\dot{\alpha}_3^2\right]^{\frac{1}{2}} \tag{29}$$

C. Acceleration Analysis

Differentiating (17) results in acceleration:

$$\left(jl_2\ddot{\alpha}_2e^{j\alpha_2} + j^2l_2\dot{\alpha}_2^2e^{j\alpha_2}\right) + \left(jl_3\ddot{\alpha}_3e^{j\alpha_3} + j^2l_3\dot{\alpha}_3^2e^{j\alpha_3}\right) - \ddot{l}_1 = 0 \tag{30}$$

Simplifying (30) results in:

$$\left(jl_2\ddot{\alpha}_2e^{j\alpha_2} - l_2\dot{\alpha}_2^2e^{j\alpha_2}\right) + \left(jl_3\ddot{\alpha}_3e^{j\alpha_3} - l_3\dot{\alpha}_3^2e^{j\alpha_3}\right) - \ddot{l}_1 = 0 \tag{31}$$

$$a_2 + a_{32} - a_1 = 0 \tag{32}$$

where a_1 is the acceleration of the slider:

$$a_2 = \left(jl_2\ddot{\alpha}_2e^{j\alpha_2} - l_2\dot{\alpha}_2^2e^{j\alpha_2}\right) \tag{33}$$

$$a_{32} = \left(jl_3\ddot{\alpha}_3e^{j\alpha_3} - l_3\dot{\alpha}_3^2e^{j\alpha_3}\right) \tag{34}$$

$$a_1 = \ddot{l}_1 = a_2 + a_{32} \tag{35}$$

Substituting Euler equivalent results in:

$$\begin{aligned} &l_2\ddot{\alpha}_2\left(j\cos\alpha_2 - \sin\alpha_2\right) - l_2\dot{\alpha}_2^2\left(\cos\alpha_2 + j\sin\alpha_2\right) \\ &+l_3\ddot{\alpha}_3\left(j\cos\alpha_3 - \sin\alpha_3\right) - l_3\dot{\alpha}_3^2\left(\cos\alpha_3 + j\sin\alpha_3\right) - \ddot{l}_1 = 0 \end{aligned} \tag{36}$$

Separating real and imaginary parts results in:

$$\ddot{l}_1 = -l_2\ddot{\alpha}_2\sin\alpha_2 - l_2\dot{\alpha}_2^2\cos\alpha_2 - l_3\ddot{\alpha}_3\sin\alpha_3 - l_3\dot{\alpha}_3^2\cos\alpha_3 \tag{37}$$

$$\ddot{\alpha}_3 = \frac{-l_2\ddot{\alpha}_2\cos\alpha_2 + l_2\dot{\alpha}_2^2\sin\alpha_2 + l_3\dot{\alpha}_3^2\sin\alpha_3}{l_3\cos\alpha_3} \tag{38}$$

The absolute acceleration of the centre of mass of link 2 results in:

$$a_{m2} = \left(j\frac{l_2}{2}\ddot{\alpha}_2e^{j\alpha_2} - \frac{l_2}{2}\dot{\alpha}_2^2e^{j\alpha_2}\right) \tag{39}$$

Substituting Euler equation and simplifying results in:

$$a_{m2} = \frac{1}{2} l_2 \left(\ddot{\alpha}_2^2 + \dot{\alpha}_2^4 \right)^{\frac{1}{2}} \tag{40}$$

The absolute acceleration of the centre of mass of link 3:

$$a_{m3} = \left(j l_2 \ddot{\alpha}_2 e^{j\alpha_2} - l_2 \dot{\alpha}_2^2 e^{j\alpha_2} \right) + \left(j \frac{l_3}{2} \ddot{\alpha}_3 e^{j\alpha_3} - \frac{l_3}{2} \dot{\alpha}_3^2 e^{j\alpha_3} \right) \tag{41}$$

Substituting Euler equation and simplifying results in:

$$a_{m3} = \begin{bmatrix} l_2^2 \left(\ddot{\alpha}_2^2 + \dot{\alpha}_2^4 \right) + l_2 l_3 \cos\left(\alpha_2 - \alpha_3 \right) \ddot{\alpha}_2 \ddot{\alpha}_3 + \\ l_2 l_3 \sin\left(\alpha_2 - \alpha_3 \right) \ddot{\alpha}_2 \dot{\alpha}_3^2 - \\ l_2 l_3 \sin\left(\alpha_2 - \alpha_3 \right) \dot{\alpha}_2^2 \ddot{\alpha}_3 + \\ l_2 l_3 \cos\left(\alpha_2 - \alpha_3 \right) \dot{\alpha}_2^2 \dot{\alpha}_3^2 + \\ \frac{1}{4} l_3^2 \left(\ddot{\alpha}_3^2 + \dot{\alpha}_3^4 \right) \end{bmatrix}^{\frac{1}{2}} \tag{42}$$

VI. Numerical Results

MATLAB software was used to describe the kinematic behaviors of the links. It was assumed that the slider crank flexible mechanism was an harmonic oscillation with the following sine function in the range of time, $t = 0 \div 0.2 \div 1.2$ s. Figs. 7-9 illustrate the position, velocity and acceleration diagrams of the slider, respectively. Figs. 10-13 show the absolute velocity and absolute acceleration of link 2 and link 3, respectively.

$$\alpha_2 = 0.3 \sin\left(25t + 60 \right) \tag{43}$$

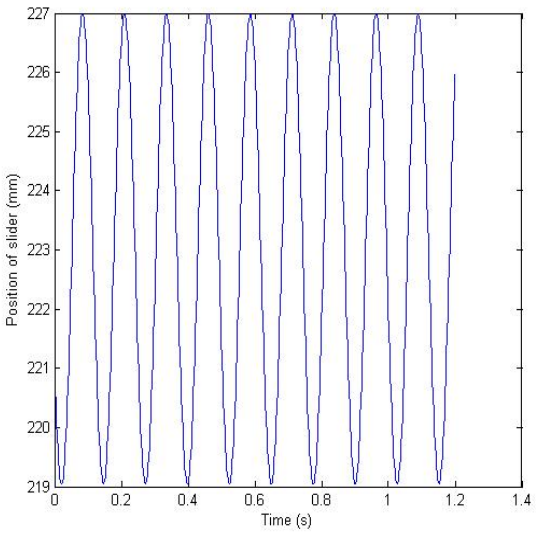

Fig. 7 Position diagram of slider

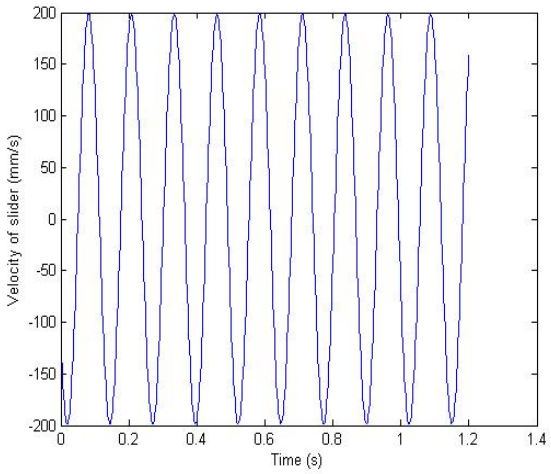

Fig. 8 Velocity diagram of slider

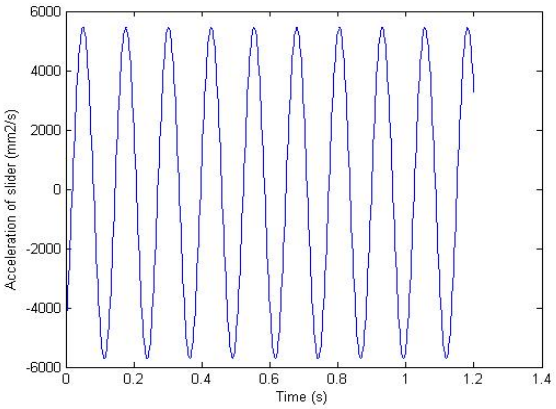

Fig. 9 Acceleration diagram of slider

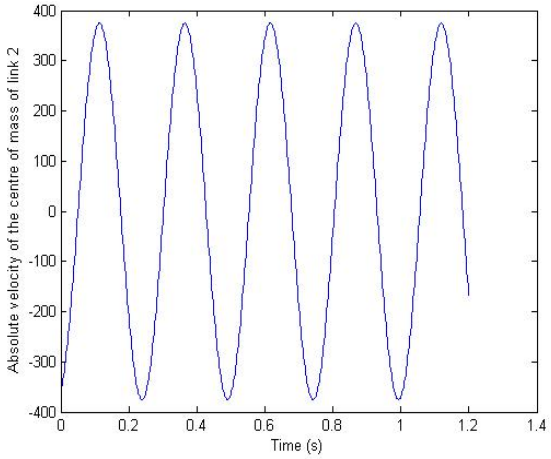

Fig. 10 Diagram of absolute velocity of centre of link 2

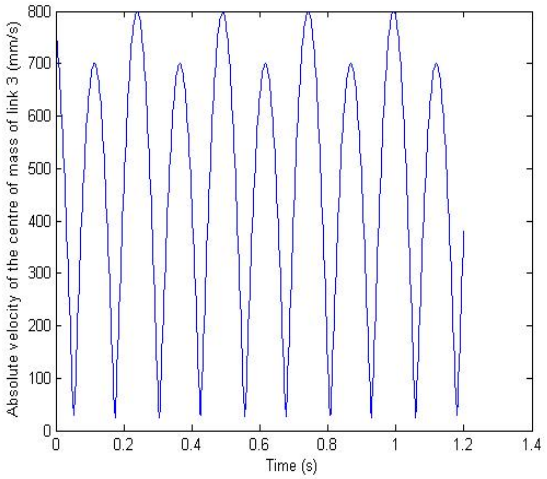

Fig. 11 Diagram of absolute velocity of centre of link 3

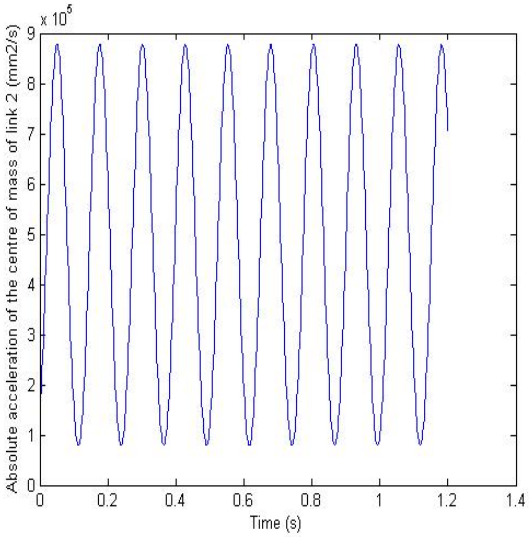

Fig. 12 Diagram of absolute acceleration of centre of link 2

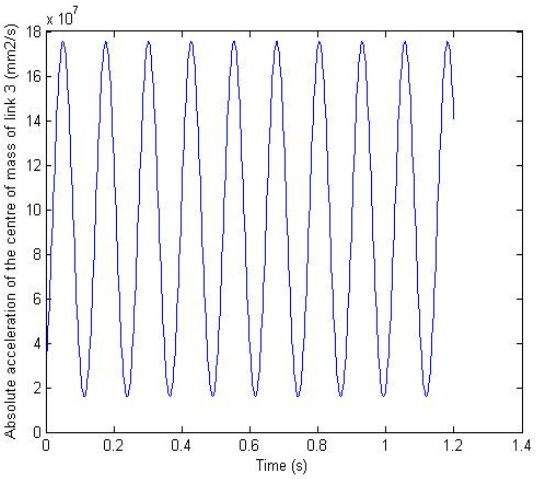

Fig. 13 Diagram of absolute acceleration of centre of link 3

VII. Finite Element Analysis and Fabrication

A non-linear finite element analysis (FEA) in ANSYS was used to predict the stress distribution of the slider crank flexible mechanism, as illustrated in Fig. 14, which shows that the maximum stress took place at the circular flexible hinge of link 2.

After the optimum conditions were determined and the kinematic responses under these conditions were also predicted, a simulation was designed and conducted with the optimum levels of the size of the proposed joint to show the maximum stress concentration. The final step was to predict and verify the fatigue life and kinematic behaviors. Thus, a prototype was made by Wire Electrical Discharge Machining, as shown in Fig. 15.

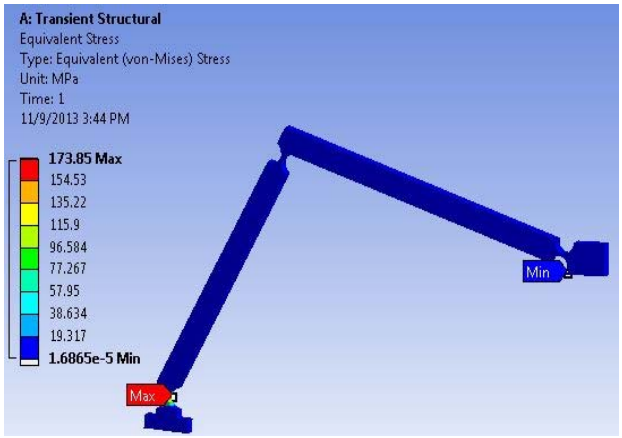

Fig. 14 Schematic diagram of stress distribution

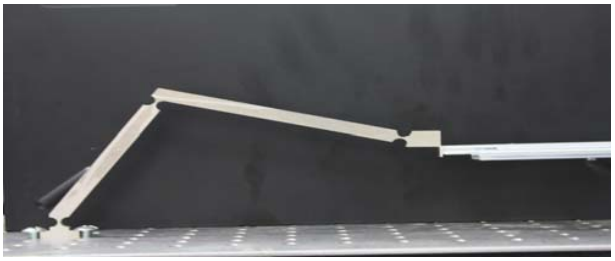

Fig. 15 Prototype of slider crank flexible mechanism prepared for kinematic and dynamic testing

VIII. Conclusion

This paper has presented an optimal design of a slider crank flexible mechanism with circular cross-section flexure hinges, an improvement over a traditional mechanism through the application of the concept of the compliant mechanism. This study focused on the structural optimization of a flexure hinge by employing the Taguchi method, with the purpose of maximizing the fatigue life of this mechanism. The input parameters were the force applied on input link 2, the width and the thickness of the flexible hinges. ANOVA was used to find the most significant parameter. Kinematic equations and behaviors were formulated and determined using PRBM and

geometric relations. MATLAB software was used to illustrate the numerical results of the kinematic behaviors.

An FEA based on ANSYS was used to illustrate the stress distribution. The optimal results as found were a force of 8.5 *N*, a width of 9 *mm* and a thickness of 1.1 *mm*. The thickness of the proposed hinge was the most significant parameter affecting the structure of the flexure hinge, with an F test of 15.5. The design and optimization approaches introduced in this study could also be applied for other similar flexure hinges. Future work will include an investigation into the location of the center of rotation and the dynamic motion of the flexible slider crank mechanism, and the analytical models will be confirmed by experiments.

ACKNOWLEDGMENT

The authors acknowledge and thank the National Science Council of the Republic of China for their financial support of this study under Contract Number: NSC 102-2221-E-151-022.

REFERENCES

[1] E. Tanık, "Transmission angle in compliant slider-crank mechanism," Mechanism and Machine Theory, vol. 46, pp. 1623–1632, 2011.
[2] F. Dirksena, M. Anselmanna, T.I. Zohdi, R. Lammering, "Incorporation of flexural hinge fatigue-life cycle criteria into the topological design of compliant small-scale devices," Precision Engineering, vol. 37, pp. 531–541, 2013.
[3] Y. Javadi, S. Sadeghi, M. A. Najafabadi, "Taguchi optimization and ultrasonic measurement of residual stresses in the friction stir welding," Materials and Design, vol. 55, pp. 27–34, 2014.
[4] H. Tari, H.J. Su, "A complex solution framework for the kinetostatic synthesis of a compliant four-bar mechanism," Mechanism and Machine Theory, vol. 46, pp. 1137–1152, 2011.
[5] Bauchau and S. Han, "Flexible joints in structural and multibody dynamics," Mech. Sci., vol. 4, pp. 65–77, 2013.
[6] L.L. Howell, Compliant Mechanisms. John Wiley and Sons Inc, New York, 2001, ch. 5.
[7] F. Dirksen and R. Lammering, "On mechanical properties of planar flexure hinges of compliant mechanisms," Mech. Sci., vol. 2, pp. 109–117, 2011.
[8] H. Gerber. Bestimmung der zulassigen spannungen in eisenkonstruktionen. Zeitschrift des Bayerischen Architeckten und Ingenieur-Vereins, vol. 6, pp. 101–10, 1874.
[9] J. Goodman. Mechanics applied to engineering. London, Longman, Green and Co., 1899.
[10] C. Soderberg. Factor of safety and working stress. Transactions of ASME, vol. 52, pp. 13–28, 1939.
[11] T.P.Dao and S.C.Huang, "Optimization of process parameters and fatigue prediction for flexure-based compliant mechanism," J. Eng. Technol. Educ., vol 10, no. 2, pp. 204-220, 2013.
[12] J.E. Shigley and C.R. Mischke, Mechanical Engineering Design, 6th ED, McGraw-Hill, New York, 2001, ch.6.

Thanh-Phong Dao received his B.Sc. degree in Mechanical Engineering from University of Technical Education Ho Chi Minh City, Vietnam in 2008. He received M.Sc. degree in Mechanical Engineering from National Kaohsiung University of Applied Sciences, in 2011. He is currently a Ph.D. student in National Kaohsiung University of Applied Sciences. His interests include compliant mechanism, optimal systems design, kinematics and dynamics, flexible manipulators.

Shyh-Chour Huang is a Professor at National Kaohsiung University of Applied Sciences. He received his Bachelor's Degree in Aeronautics and Astronautics Engineering from the National Cheng-Kung University in 1980, Taiwan, ROC. He received his PhD in Mechanical Engineering from the University of Cincinnati, USA in 1990. His research interests include micro-electro-mechanical systems design, biomechanics and multibody dynamics.